Organic &
Biomolecular Chemistry

Dynamic Article Links ►

Cite this: DOI: 10.1039/c0xx00000x

PAPER

www.rsc.org/xxxxxx

Inhibition Studies on *Mycobacterium tuberculosis N*-acetylglucosamine-1-phosphate uridyltransferase (GlmU)

Anh Thu Tran[a], Daying Wen[b], Nicholas. P. West[c], Edward N. Baker,[b] Warwick J. Britton[c] and Richard J. Payne*[a]

Received (in XXX, XXX) Xth XXXXXXXXX 20XX, Accepted Xth XXXXXXXXX 20XX
DOI: 10.1039/b000000x

Peptidoglycan is an essential component of the cell wall of bacteria, including *Mycobacterium tuberculosis*, that provides structural strength and rigidity to enable internal osmotic pressure to be withstood. The first committed step in the biosynthesis of peptidoglycan involves the formation of uridine diphosphate-*N*-acetylglucosamine (UDP-GlcNAc) from uridine triphosphate (UTP) and GlcNAc-1-phosphate. This reaction is catalysed by *N*-acetylglucosamine-1-phosphate uridyltransferase (GlmU), a bifunctional enzyme with two independent active sites that possess acetyltransferase and uridyltransferase activities. Herein, we report the first inhibition study targeted against the uridyltransferase activity of *M. tuberculosis* GlmU. A number of potential inhibitors were initially prepared leading to the discovery of active aminoquinazoline-based compounds. The most potent inhibitor in this series exhibited an IC_{50} of 74 μM against GlmU uridyltransferase activity and serves as a promising starting point for the discovery of more potent inhibitors.

Introduction

Tuberculosis (TB), caused by infection with the bacterium *Mycobacterium tuberculosis* has remained a major global health risk since the first identification of the disease in 1882.[1] According to the World Health Organization, in 2011 there were 8.3 million new reported cases of TB and 1.4 million deaths as a result of the disease.[2] A major challenge for TB treatment is the persistent nature of *M. tuberculosis* where the bacterium is capable of residing in a dormant state in very low numbers for decades after the initial infection.[1] This results in a lifelong risk of disease reactivation especially in immune compromised patients such as those co-infected with human immunodeficiency virus (HIV).[1] To effectively combat the persistency of *M. tuberculosis*, a combination therapy comprising of four frontline antibiotics (rifampicin, isoniazid, ethambutol and pyrazinamide) for a period of 6-9 months is employed.[3, 4] However, poor adherence to this treatment regimen has contributed to the emergence of multi-drug resistant (MDR) TB, which requires the use of second line therapies, and extensively drug resistant (XDR) TB, for which there is no effective treatment in many resource limited countries.

Given the increased incidence of drug resistant TB cases worldwide, there is a desperate need for the development of new anti-tubercular agents that operate *via* novel modes of action to the currently employed drugs. A very successful avenue for anti-tubercular development has involved the development of compounds that target enzymes responsible for the biosynthesis and assembly of the mycobacterial cell wall. Examples include currently employed first and second-line TB drugs such as isoniazid, ethambutol and ethionamide.[5] These agents act by disrupting the biosynthesis or the incorporation of mycolic acid, a key lipid which constitutes a major component of the mycobacterial cell wall (Figure 1).[5]

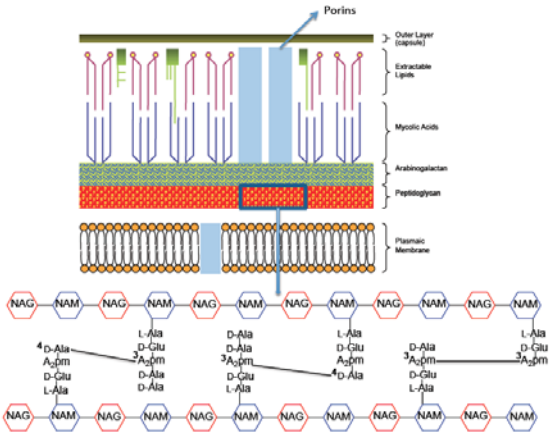

Figure 1. A schematic of the *M. tuberculosis* cell envelope showing the arrangement of key components; mycolic acids, arabinogalactan and peptidoglycan and porins. The peptidoglycan layer is enlarged (below) depicting classical 4→3 and non-classical 3→3 interpeptide bonds. NAM: *N*-acetylmuramic acid; NAG: *N*-acetylglucosamine; A_2pm: *meso*diaminopimelate.[6]

Another essential component of the mycobacterial cell wall is the peptidoglycan layer which provides structural strength and rigidity to the bacterium to withstand internal osmotic pressure. Structurally, peptidoglycan consists of a repeating unit of *N*-acetylglucosamine (NAG) and *N*-acetylmuramic acid (NAM) bearing crosslinked peptide bridges (Figure 1).[7] Whilst peptidoglycan biosynthesis has been an extremely successful drug target for both gram-positive and gram-negative bacteria, enzymes responsible for the construction of this structure in mycobacteria have not been extensively investigated as drug targets. This is in part due to the well-established broad-spectrum β-lactamase (BlaC) activity of *M. tuberculosis* that inactivates traditional β-lactam antibiotics.[4, 8, 9] However, other enzymes responsible for the biosynthesis of peptidoglycan remain viable TB drug targets. Indeed, following the publication of the *M. tuberculosis* genome in 1998[10], a number of enzymes responsible for the biosynthesis of peptidoglycan have been elucidated thereby providing new targets for the development of anti-tubercular lead compounds that operate *via* novel modes of action. One such target is *N*-acetylglucosamine-1-phosphate uridyltransferase (GlmU).[11, 12] This bi-functional enzyme, found exclusively in bacteria, is responsible for catalysing the formation of UDP-GlcNAc, an important intermediate in the biosynthesis of peptidoglycan in *M. tuberculosis*.[11] Importantly, a crystal structure of *M. tuberculosis* GlmU has recently been solved which has provided important insights into the two active sites of the enzyme.[11]

The bifunctional role of GlmU arises from two independent domains of the enzyme which possess acetyltransferase and uridyltransferase activities.[11] The acetyltransferase domain, found in the C-terminus of the protein is responsible for the first step of the reaction, in which an acetyl group is transferred from AcCoA to GlcN-1-P forming GlcNAc-1-P.[11] GlcNAc-1-P then serves as a substrate for the uridyltransferase active site in the *N*-terminus of the enzyme which forms UDP-GlcNAc (Scheme 1).[11] Structurally, the *C*-terminus of the protein adopts a regular left-hand β-helix while the *N*-terminus exhibits a Rossmann fold topology (Scheme 1B).[11] It has been proposed that the mechanism of *M. tuberculosis* GlmU catalysis first involves UTP and Mg^{2+} binding to the uridyltransferase active site prior to GlcNAc-1-P binding in the adjacent pocket.[11, 13] Upon GlcNAc-1-P binding, the enzyme undergoes major conformational changes to facilitate uridylation which begins with nucleophilic attack by the phosphate group of GlcNAc-1-P at the α-phosphate of UTP thus forming a pentacoordinate intermediate stabilised by the Mg^{2+} cation (Scheme 1A).[11, 13] The final steps involve inversion of stereochemistry at the α-phosphate and the release of pyrophosphate (Scheme 1A).[11, 13]

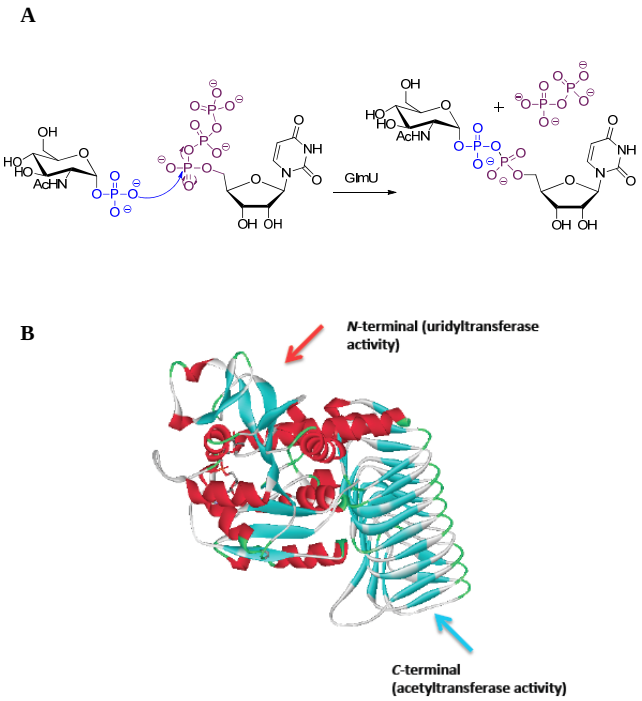

Scheme 1. **A.** Mechanism of uridylation by GlmU. **B.** Structure of *M. tuberculosis* GlmU showing the *C*-and *N*-terminal catalytic domains.[11]

Inhibitors of the *Haemophilus influenzae* and *Trypanosoma brucei* GlmU isozymes were recently identified by high-throughput screening with some compounds exhibiting IC_{50} values in the low to mid-micromolar range.[14-16] To date, however, no inhibitors have been reported for the *M. tuberculosis* enzyme. Herein we report the first inhibition study against *M. tuberculosis* GlmU. Since the uridyltransferase activity is proposed to be the rate-limiting step of the two catalytic processes (as hypothesised through kinetic modeling studies) we chose to target the uridyltransferase activity of the enzyme in this work.[17]

Results and Discussion

GlmU uridyltransferase kinetic assay

Prior to the design of GlmU uridyltransferase inhibitors, we first embarked on the development of a continuous kinetic assay for *M. tuberculosis* GlmU uridyltransferase. To this end, a double-enzyme-coupled continuous assay was developed based on an assay originally reported by Webb and co-workers which monitors the formation of inorganic pyrophosphate.[18, 19]

Specifically, this assay used excess amounts of two coupling enzymes, namely inorganic pyrophosphatase (EC 3.6.1.1) and purine nucleoside phosphorylase (EC 2.4.2.1) in the presence of 2-amino-6-mercapto-7-methylpurine ribonucleoside (MESG).[18, 19] In this double coupled enzyme assay, the pyrophosphate produced by GlmU uridyltransferase is subsequently hydrolysed to inorganic phosphate by inorganic pyrophosphatase. The inorganic phosphate then serves as a substrate for purine nucleoside phosphorylase which catalyses the phosphorolytic cleavage of the glycosidic bond in MESG (λ_{max} = 330 nm), resulting in the formation of 2-amino-6-mercapto-7-methylpurine (λ_{max} = 360 nm) that can be detected spectroscopically (Scheme 2).[18, 19]

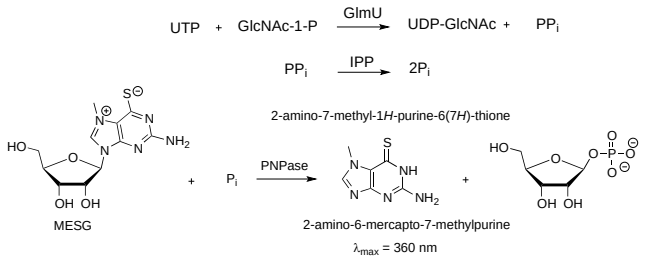

Scheme 2. Double-enzyme-coupled *M. tuberculosis* GlmU uridyltransferase assay.

During the development of the GlmU uridyltransferase kinetic assay, a number of variables including the concentrations of *M. tuberculosis* GlmU and MESG and assay temperature were modified to identify the optimal assay conditions. In addition, experiments to confirm that the coupling enzymes, inorganic pyrophosphatase and purine nucleoside phosphorylase, were not rate-limiting and that the assay was directly measuring the activity of GlmU uridyltransferase were performed (see Supplementary Information). These studies were further supported by a linear dependence of reaction rate on GlmU uridyltransferase concentration (see Supplementary Information).

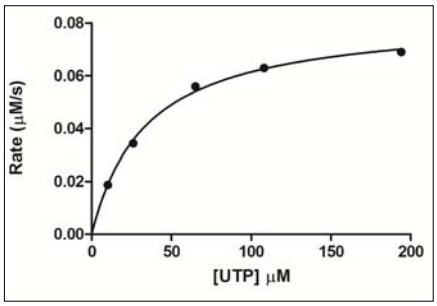

Figure 2. Least square fitted curve to the Michaelis-Menten model for *M. tuberculosis* GlmU uridyltransferase ($K_{M\ UTP}$ = 34 ± 3 μM, V_{max} = 0.082 ± 0.002 μM s^{-1}, [GlcNAc-1-P] = 1 mM).

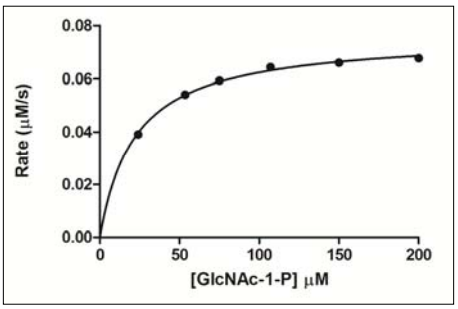

Figure 3. Least square fitted curve to the Michaelis-Menten model for *M. tuberculosis* GlmU uridyltransferase ($K_{M\ GlcNAc-1-P}$ = 22 ± 1 μM, V_{max} = 0.076 ± 0.001 μM s^{-1}, [UTP] = 1 mM).

The optimized assay was subsequently used for the determination of kinetic parameters for both UTP and GlcNAc-1-P as substrates for GlmU activity whereby the apparent K_M and V_{max} values for one substrate were determined at a saturating concentration (1 mM) of the other substrate (Figure 2 and 3).

Design of bisubstrate and transition-state based inhibitors of GlmU uridyltransferase

Following the development of the coupled continuous kinetic assay for *M. tuberculosis* GlmU uridyltransferase, we next embarked on the design and synthesis of inhibitors of this enzyme. The substrates and putative transition state of the GlmU uridyltransferase reaction were used as starting points for inhibitor design. To begin with, two transition-state mimics were designed and synthesised (compounds **1** and **2**, Figure 4A). Compound **1** featured a di-carboxylate moiety capable of co-ordinating to the catalytic Mg^{2+} in a similar manner to the phosphate motif in the transition state. In contrast, compound **2** possessed a 2,3-dihydroxybenzamide moiety which was designed to serve as a surrogate for the leaving pyrophosphate group (Figure 4A). Unfortunately, despite the incorporation of characteristic transition state features of the proposed GlmU uridyltransferase reaction, these compounds only exhibited weak inhibition against the enzyme (10% and 60% inhibition at 2 mM, Figure 4A).

In addition to the above transition-state mimics, we also designed bisubstrate inhibitors containing structural features of both GlcNAc-1-P and UTP. Compound **3** possessed an α-linked GlcNAc moiety while **4** contained a GlcNAc mimicking catechol unit. Each of these compounds also featured a uridine motif with a sulfonamide or aminothiazole bridge. The sulfonamide linker was chosen as this functionality has been successfully used as a phosphate bioisostere[20] while the aminothiazole moiety was successfully employed by Kiessling and co-workers[21] as a pyrophosphate shape mimic in the development of UDP-galactopyranose mutase inhibitors. Unfortunately, both sulfonamide and aminothiazole-based compounds demonstrated weak inhibition of *M. tuberculosis* GlmU uridyltransferase activity (**3**: 55% inhibition at 2 mM, **4**: 37% inhibition at 2 mM, Figure 4B).

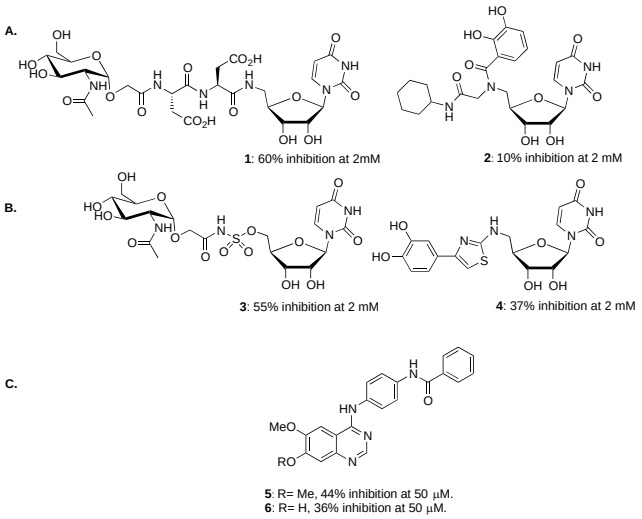

Figure 4. First generation *M. tuberculosis* GlmU uridyltransferase inhibitors.

In parallel with our transition-state and bisubstrate inhibitor design strategy, we also synthesised aminoquinazoline-based inhibitors **5** and **6** (Figure 4C) which were identified in a recent high-throughput screen against *H. influenzae* GlmU uridyltransferase by Doig and co-workers from AstraZeneca (see Supplementary Information for synthesis).[14] These compounds exhibited promising activity when screened against *M. tuberculosis* GlmU uridyltransferase. Specifically, compound **5** exhibited 44% inhibition of the uridytransferase activity at 50 μM while compound **6** was slightly less potent with 36% inhibition at the same concentration (Figure 4C). It should be noted that while this represents a significant drop in activity compared to that observed against *H. influenzae* GlmU uridyltransferase, the *M. tuberculosis* GlmU *N*-terminal domain only possesses 41% sequence identity to the *H. influenzae* isozyme. It is also important to note that strong absorption of the aminoquinazoline compounds at λ = 360 nm meant that the assays could not be conducted with inhibitor concentrations above 50 μM.

Encouraged by the activity of analogues **5** and **6**, we embarked on the design and synthesis of an aminoquinazoline-based inhibitor library using the more potent 6,7-dimethoxyquinazoline inhibitor **5** as a starting point to explore structure-activity relationships against *M. tuberculosis* GlmU uridyltransferase. The general strategy for structural modifications of compound **5** is summarised in Figure 5. Our SAR exploration was focused on the sequential evaluation of the role and relative importance of the central 1,4-phenylenediamine linker, the terminal phenyl group and the bicyclic dimethoxyquinazoline scaffold.

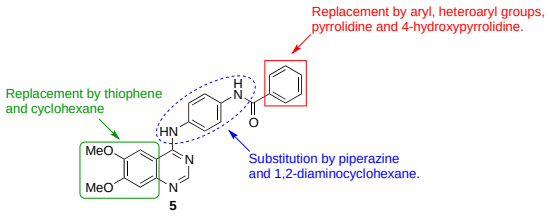

Figure 5. Proposed structural modifications of inhibitor **5**.

Our initial investigation focused on the evaluation of the importance of the terminal phenyl group and the central 1,4-phenylenediamine linker in **5**. To this end, we proposed to replace the phenyl moiety of aminoquinazoline-based inhibitor **5** with cyclohexane, pyrrolidine and 4-hydroxypyrrolidine, while piperazine and 1,2-diaminocyclohexane linkers were employed to substitute the 1,4-phenylenediamine moiety in **5**. These groups were introduced to evaluate the effect of incorporating hydrogen bond donors and acceptors as well as conformational flexibility into the terminal group and the central linker on GlmU uridyltransferase inhibitory activity. Compounds lacking the terminal phenyl group were also synthesised to assess the contribution of this functionality on inhibitory activity.

Synthesis of aminoquinazoline GlmU uridyltransferase inhibitors

Synthesis of a series of aminoquinazoline GlmU inhibitors began with 2-amino-4,5-dimethoxybenzoic acid **7**. Condensation of **7** with ammonium acetate and trimethyl orthoformate afforded quinazolinone intermediate **8** in 85% yield (Scheme 3). Reaction of **8** with phosphorus(V) oxychloride then provided the corresponding chloroquinazoline **9** which was subsequently subjected to S_NAr reactions with 1,4-phenylenediamine, piperazine and racemic *trans*-1,2-diaminocyclohexane respectively to afford amines **10**-**12** in good yields (Scheme 3).

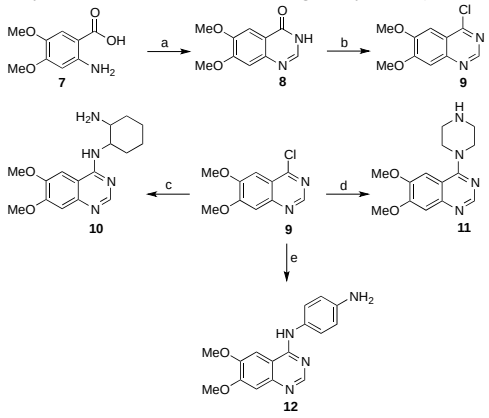

Scheme 3. Synthesis of amines **10**-**12**. *Reagents and conditions*: a) $CH(OMe)_3$, NH_4OAc, MeOH, 120 ºC, 3 h, 85%; b) $POCl_3$, 110 ºC, 5 h, 70%; c) (±)-*trans*-1,2-diaminocyclohexane, 2-propanol, 110 ºC, 3 h, 60%; d) piperazine hydrochloride hydrate, 2-propanol, 110 ºC, 3 h, 70%; e) 1,4-phenylenediamine, 2-propanol, 110 ºC, 3 h, 85%.

Amines **10**-**12** were subsequently coupled with a variety of carboxylic acids using either *N*,*N*'-diisopropylcarbodiimide (DIC) or O-(7-azabenzotriazol-1-yl)-*N*,*N*,*N*',*N*'-tetramethyluronium hexafluorophosphate (HATU) as coupling reagents to afford inhibitors **13**-**17** in 37-50% yield (Scheme 4A-4C). The *tert*-butyl

carbamate of **18** was removed by treatment with 4 M HCl in dioxane to provide inhibitor **19** (Scheme 4D).

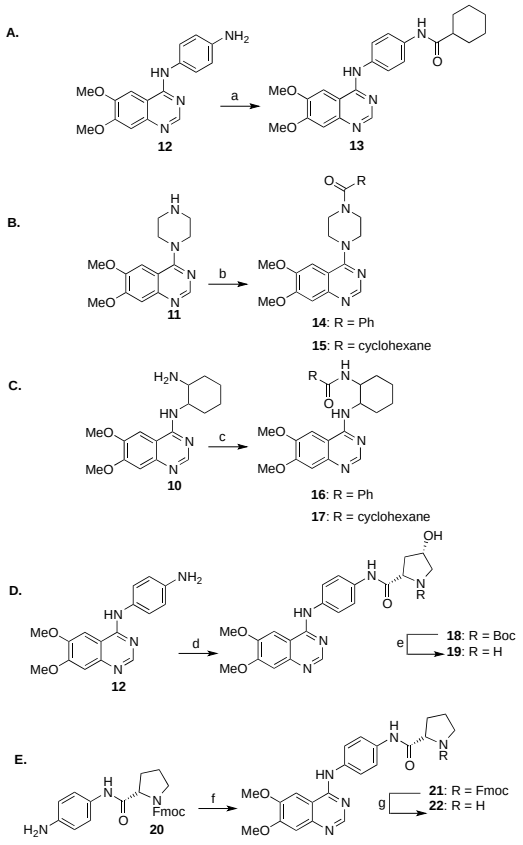

Scheme 4. Synthesis of inhibitors **13**-**18**, **19**, **22**. *Reagents and conditions*: A. a) **13**: Cyclohexane carboxylic acid, DIC (2 eq.), DMAP (2 eq.), DMF, rt, 20h, 56%; B. b) **14**: Benzoic acid, HATU (1.5 eq.), *i*Pr_2NEt (1.5 eq.), DMF, rt, 4 h, 47%; **15**: Cyclohexane carboxylic acid, HATU (1.5 eq.), *i*Pr_2NEt (1.5 eq.), DMF, rt, 20 h, 50%; C. c) **16**: Benzoic acid, HATU (1.5 eq.), *i*Pr_2NEt (1.5 eq.), DMF, rt, 4 h, 30%; **17**: Cyclohexane carboxylic acid, HATU (1.5 eq.), *i*Pr_2NEt (1.5 eq.), DMF, rt, 24 h, 31%; D. d) **18**: Boc-L-Hyp-OH, HATU (1.5 eq.), *i*Pr_2NEt (1.5 eq.), DMF, rt, 20 h; e) **19**: 4 M HCl in dioxane, rt, 16 h, 30% over 2 steps. E. f) **21**: Chloroquinazoline **9**, 2-propanol, 110 ºC, 3 h; g) **22**: 25% piperidine, CH_2Cl_2: MeOH (1:1, v/v), rt, 30 min, 25% over 2 steps.

As a result of solubility problems in the coupling reaction, a modified procedure was required for the preparation of the proposed inhibitor bearing an unsubstituted pyrrolidine terminal group. An S_NAr reaction between (*S*)-*N*-(4-aminophenyl)pyrrolidine-2-carboxamide fragment **20** (see Supplementary Information for synthesis) and chloroquinazoline **9** to initially provide Fmoc-protected aminoquinazoline **21** (Scheme 4E). Deprotection of the Fmoc-carbamate using 25% piperidine (vol/vol) in a mixture of methanol and dichloromethane (1:1 v/v) afforded inhibitor **22** in moderate yield over two steps.

GlmU uridyltransferase inhibition studies

With the first series of 11 inhibitors in hand, we next evaluated these compounds for their inhibitory activity. To this end, compounds **13-18**, **19 and 22** were screened against *M. tuberculosis* GlmU uridyltransferase using the double-coupled continuous kinetic assay described above. The inhibition assays were carried out at fixed concentrations of UTP and GlcNAc-1-P ([UTP] = 35 μM and [GlcNAc-1-P] = 35 μM) in the presence of the inhibitors at 50 μM. Unfortunately, as with parent compounds, we were unable to obtain IC_{50} values for the majority of compounds owing to the combination of low solubility at high concentrations (>200 μM) and high absorbance (at λ = 360 nm) at concentrations that were required for determining an accurate IC_{50} value.

After screening the 1,4-phenylenediamine-linked series of inhibitors (**5**, **12**, **13**, **19** and **22**), it was clear that the terminal phenyl group is essential for inhibition of GlmU uridyltransferase activity (Table 1). This is emphasised by the substitution of the phenyl group in **5** with a cyclohexane moiety in **13** which resulted in a two-fold decrease in inhibition (**5**: 44% inhibition at 50 μM and **13**: 22% inhibition at 50 μM, Table 1). Similarly, removal of this group in **12** led to a three-fold drop in potency (**12**: 14% inhibition at 50 μM, Table 1). Replacement of the terminal phenyl group in **5** with pyrrolidine and hydroxypyrrolidine in **19** and **22** respectively, also resulted in reduced inhibition of GlmU uridyltransferase activity (8% inhibition at 50 μM for **19** and **22**). Replacement of the rigid 1,4-phenylenediamine linker in **5** and **13** with piperazine (**14** and **15**) and 1,2-diaminocyclohexane linkers (**16** and **17**) also resulted in a substantial decrease in activity, suggesting that precise positioning of terminal groups is necessary for optimal interactions with GlmU uridyltransferase active site residues. Piperazine-linked inhibitor **14** bearing a terminal phenyl ring only exhibited 14% inhibition at 50 μM compared to 44% inhibition at 50 μM for **5** (Table 1). Similar to the observation in the 1,4-phenylenediamine series, replacement of the phenyl moiety in **14** with cyclohexane in **15** led to a further decrease in enzyme inhibition. This decrease was even more pronounced in the 1,2-diaminocyclohexane-linked compounds **16** and **17** in which no inhibition of GlmU uridyltransferase activity was observed at 50 μM (Table 1). This result suggests the importance of the 1,4-substitution of the linker unit for optimal activity.

Given the superiority of the rigid 1,4-phenylenediamine linker over more flexible linkers, we decided to retain this linker in a second-generation series of GlmU uridyltransferase inhibitors. In order to identify the optimal terminal group for the 1,4-phenylenediamine linked inhibitors, a large range of aryl moieties with varied electronic and steric properties were incorporated *via* the previously established synthetic route (Scheme 5).

Table 1. Inhibition of uridyltransferase activity of *M. tuberculosis* GlmU by aminoquinazoline inhibitors with variation in linker and terminal groups.

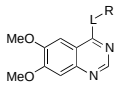

Compound	Linker (L)	R	% inhibition at 50 μM
5	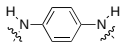		44%
13	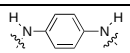		22%
12	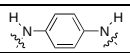	H	14%
19	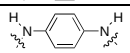	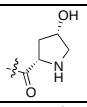	8%
22	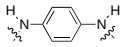		8%
11		H	No inhibition
14			14%
15			No inhibition
10		H	No inhibition
16			No inhibition
17			No inhibition

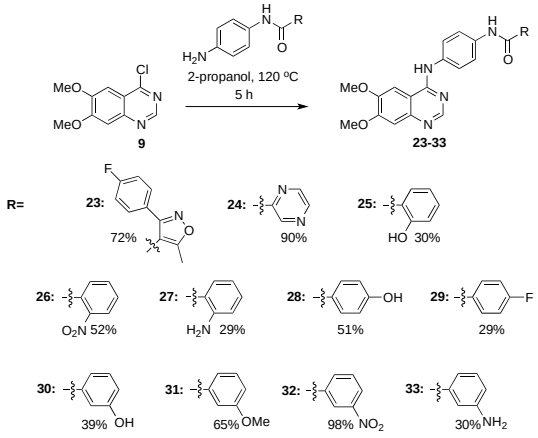

Scheme 5. Synthesis of inhibitors **23-33** *via* a S_NAr route.

From previous inhibition study against *H. influenzae* GlmU, it was established that the terminal benzamide group in inhibitor **5** occupied the lipophilic pocket adjacent to the GlcNAc binding subsite. Sequence alignment of lipophilic pocket residues of *H. influenzae* GlmU (A217-V223, L129-133 and V168-T170) and *M. tuberculosis* GlmU (V229-V235, V139-T143 and V180-A182) revealed that many amino acid residues in this region are not highly conserved. As such, we decided to probe the interactions made with the lipophilic pocket of *M. tuberculosis* GlmU by incorporating steric bulk in the terminal group. Initial studies incorporating hydrophobic moieties resulted in compounds with low solubility under our enzyme assay conditions (not shown). However, 4-fluorophenylisoxazole-based inhibitor **23** could be solubilised to a concentration of 50 μM, however this modification resulted in a two-fold decrease in potency compared to **5**. This suggests that extension of the terminal aryl moiety is not well accommodated in the lipophilic pocket of *M. tuberculosis* GlmU. Substitution of the terminal phenyl ring in **5** with pyrazine in **24** resulted in reduced potency against GlmU uridyltransferase (**24**: 19% at 50 μM and **5**: 44% at 50 μM) as did the introduction of a range of both electron-donating and electron-withdrawing *ortho* and *para* substituents into the terminal phenyl ring in **25-29** (13-21% at 50 μM). However, substitution at the *meta* position of the terminal phenyl ring was well-tolerated with inhibitors bearing *m*-hydroxyphenyl **30** and *m*-methoxyphenyl **31** moieties similarly potent to lead compound **5** with 38% and 35% inhibition at 50 μM, respectively. In contrast to the vast majority of inhibitors synthesised in this study, for compound **30**, we were able to determine an IC_{50} value due to the solubility at high concentrations in the assay conditions (1% DMSO in water, IC_{50} = 74 ± 1 μM). Introduction of other *meta* substituents such as nitro and amino groups (compounds **32** and **33** respectively) into the terminal phenyl ring of **5** led to diminished inhibitory activity.

Given that *m*-hydroxy substituted compound **30** was equipotent to lead compound **5**, we were next interested in probing whether larger substituents could be accommodated in this region. To this end, cyanomethyl and carboxymethyl groups were appended to the *m*-hydroxyl of **30**, to investigate the possibility of hydrogen bonding and ionic interactions in this region (Scheme 6). Surprisingly, compound **34** with a cyanomethyl group did not exhibit any inhibition at 50 μM while compound **35**, containing a carboxymethyl extension was equipotent to the unfunctionalised inhibitor **30**. In the absence of an enzyme-inhibitor co-crystal structure it is difficult to rationalize the differing activity of these two compounds. Future work in our laboratories will therefore involve the co-crystallisation of inhibitors described in Table 2 with *M. tuberculosis* GlmU to quantify the binding mode in the uridyltransferase active site to facilitate structure-based inhibitor design.

Table 2. Inhibition of uridyltransferase activity of *M. tuberculosis* GlmU by aminoquinazoline inhibitors with varied terminal aryl groups.

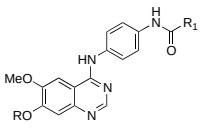

Compound	R	R_1	% Inhibition at 50 μM
23	Me	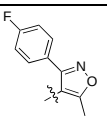	19%
24	Me		19%
25	Me		14%
26	Me		13%
27	Me		16%
28	Me	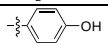	18%
29	Me	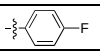	21%
30	Me		35% (IC_{50} = 74 ± 1 μM)
31	Me	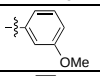	38%
32	Me	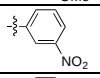	No inhibition
33	Me	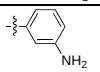	17%
34	Me	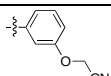	No inhibition
35	Me	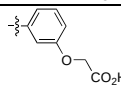	34%

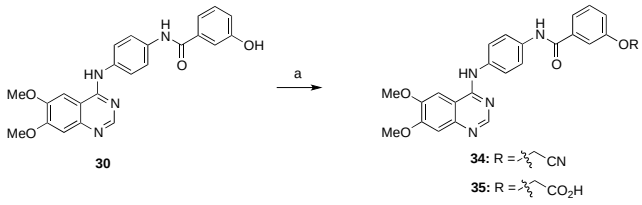

Scheme 6. Synthesis of cyanomethyl and carboxymethyl compounds **43** and **44**. *Reagents and conditions*: a) **34**: Bromoacetonitrile (1.1 eq.), Cs_2CO_3 (2.5 eq.), MeCN, 80 ºC, 1 h, 55%; **35**: *tert*-Butyl bromoacetate (1.3 eq.), Cs_2CO_3 (2.6 eq.), MeCN, 50 ºC, 3 h followed by TFA:CH_2Cl_2 (1:1 v/v), 16 h, rt, 14% over 2 steps.

Having established *m*-hydroxylphenyl as a suitable terminal group (on the basis of potency and solubility profile), we next turned our attention to the two methoxy substituents on the quinazoline ring. To this end, inhibitors **36** and **37**, in which the dimethoxyphenyl moiety in **30** was replaced by thiophenyl (**36**) and cyclohexanyl (**37**) moieties, were synthesised (See Supplementary Information for synthesis). Compound **36** exhibited comparable inhibitory activity against GlmU uridyltransferase activity as **30** (**36**: 38% compared to **30**: 35% inhibition at 50 μM, Table 3). Inhibitor **37**, bearing a cyclohexyl ring was slightly less potent (**37**: 29% inhibition at 50 μM, Table 3). While preliminary, the above results indicate that although the methoxy groups were not essential for inhibition of GlmU uridyltransferase, the planarity of the quinazoline ring may contribute to the binding of inhibitors to the active site of GlmU uridyltransferase. These results are in stark contrast with those obtained for the *H. influenzae* enzyme by Doig and co-workers.[14] Specifically, the co-crystal structure of the aminoquinazoline-based inhibitor **6** bound to *hi*GlmU uridyltransferase revealed an important hydrogen bonding interaction between the C-7 hydroxyl of the quinazoline ring with the amide backbone of an alanine residue (A13 in *hi*GlmU uridyltransferase). It was proposed that this hydrogen bonding interaction mimicks the interaction made by the C-2 carbonyl of the uridine moiety in the substrate (UTP). In light of the above results, it is therefore possible that the aminoquinazoline inhibitors synthesised here exhibit different binding modes to *M. tuberculosis* GlmU compared to the *hi*GlmU homologue. These results also offer the possibility of further structural modifications in future inhibition studies.

At this point, we were also interested in the arrangement of hydrogen bond donor and acceptor moieties in the amide linker that bridges the central motif with the terminal groups. To this end, we prepared compound **38** with a reverse amide linker (see Supplementary Information for synthesis) and surprisingly, this compound showed a remarkable decrease in inhibition of GlmU (**38**: 7% at 50 μM, **30**: 35% at 50 μM), suggesting that the alignment of hydrogen bond donors and acceptors in the amide linker region may be important for inhibition of the enzyme.

Table 3. Inhibition of uridyltransferase activity of *M. tuberculosis* GlmU by inhibitors with variation in the aminoquinazoline core or central amide linker.

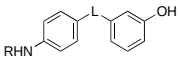

Compound	R	L	% Inhibition at 50 μM
36			38%
37			30%
38	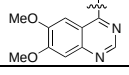		7%

The above aminoquinazoline-based inhibitors were also screened for activity against virulent *M. tuberculosis* (strain H37Rv) to assess the potential of these compounds as TB drug leads using the well-established microplate-based assay with Alamar blue (resazurin) readout (MABA).[22] Unfortunately, most compounds did not exhibit anti-tubercular activity with the exceptions of compound 6 and 17 exhibiting an MIC_{50} of 200 μM.

Conclusions

In summary, we have developed a continuous double coupled kinetic assay *for M. tuberculosis* GlmU uridyltransferase and successfully synthesised the first micromolar inhibitors against this enzyme. These inhibitors will serve as useful tools for enzyme co-crystallisation studies which will provide important information on the interactions necessary for potent inhibition of *M. tuberculosis* GlmU uridyltransferase. Experiments towards this goal are currently underway in our laboratories and will be reported in due course.

Notes and references

[a] *School of Chemistry, Building F11, The University of Sydney, Camperdown, NSW, 2006, Australia. Fax: 61 29351 3329; Tel: 61 29351 5877; E-mail: richard.payne@sydney.edu.au*

[b] *Maurice Wilkins Centre for Molecular Biodiscovery and Laboratory of Structural Biology, School of Biological Sciences, University of Auckland, Auckland, 1010, New Zealand*

[c] *Centenary Institute, Newtown, NSW, 2042, Australia and Sydney Medical School, University of Sydney. NSW 2006, Australia.*

† Electronic Supplementary Information (ESI) available: experimental procedures for compounds **1**-**4** and **36**-**38**, ^{1}H and ^{13}C NMR spectra of all novel compounds and results for GlmU assay optimisation studies. See DOI: 10.1039/c0xx00000x.

Experimental

Biological Experimental

Expression and Purification of *M. tuberculosis* GlmU uridyltransferase

The *glmU* gene was amplified from *M. tuberculosis* genomic DNA by PCR using the primers 5' GGCAGCGGCGCGATGACGTTTCCTGGTGACAC-3' and 5' GAAAGCTGGGTGTCACGGTGTCTGATCAGC-3'. The construct was cloned into the pDEST17 N-terminal His6-tag vector (Invitrogen) using Gateway cloning. The GlmU protein was overexpressed in *E. coli* BL21(DE3) cell strain using an autoinduction protocol.[23] An overnight culture was prepared by inoculating 5 mL PA-0.5G medium supplemented with ampicillin (100 mg/mL) and incubating at 37 ºC with shaking (180 rpm/min). Overnight cultures were transferred into 1 L ZYP-5052 medium and incubated at 37 ºC with shaking at 180 rpm/min. On reaching an OD600 of 0.7 (approximately 4 h), the cell culture was cooled to 4 ºC for 1 h. The culture was then incubated for approximately 18 h at 18 ºC with shaking at 180rpm/min. Cells were harvested by centrifugation at 5000g for 10 min at 4 ºC and resuspended in buffer A (25 mM NaH_2PO_4/Na_2HPO_4 pH 7.5, 100 mM NaCl, 14 mM β mercaptoethanol, 20mM imidazole). Cells were lysed by cell disruption (Constant Cell Disruption System) and the lysate was centrifuged at 16000 rpm/ min for 40 min. The supernatant was applied onto an immobilized metal (Ni^{2+}) affinity column (IMAC) pre-equilibrated with buffer A. A linear imidazole gradient (0–1 M) was used to elute the fusion protein. The His6 tag was cleaved by incubation with recombinant tobacco etch virus (rTEV) protease (overnight at 4 ºC), after which the rTEV protease and uncleaved protein were removed by a second IMAC step. In a final purification step GlmU was applied onto a size-exclusion column (Hi Load 16/60 Superdex 200, GE Healthcare) equilibrated with buffer B (50mM HEPES, pH 7.5, 100mM NaCl, 1mM DTT, 1mM EDTA). Purified GlmU protein was concentrated to 15mg/mL and stored in -80 ºC freezer. Purified by *M. tuberculosis* GlmU uridyltransferase has a specific activity of 2.0 units/mg of protein.

M. tuberculosis GlmU uridyltransferase assays

In 96-well plate format, the standard inhibition assay of 200 µL contained the following (50 mM Tris.HCl (pH 7.6), 5 mM $MgCl_2$, 1 mM DTT, 0.2 mM 7-methyl-6-thioguanosine (MESG), 1 U/mL purine nucleoside phosphorylase (PNPase), 2.4 U/mL inorganic pyrophosphatase, 94 nM *M. tuberculosis* GlmU uridyltransferase, 35 µM GlcNAc-1-P and 50 µM of a given inhibitor (dissolved in DMSO and water mixture with a final concentration of 1% DMSO in assay) with the exception of inhibitor **30** for which a range of concentrations were used (0-400 µM) . The assay mix was incubated, in duplicate at 25 ºC for 10 minutes prior to initiation by the addition of 35 µM UTP and monitored for 6 minutes at 360 nm on a Polarstar-Omega (BMG LabTech) microplate reader. The IC_{50} value for **30** was determined by non-linear regression fitting to the sigmoidal Hill equation (below) using GraphPad Prism (version 5.03 for Windows). where v_i/v_o is the initial fractional velocity, A and B represent top and bottom of curve, l is the logarithm of inhibitor concentration and h is Hill slope.

$$\frac{v_i}{v_o} = B + \frac{A-B}{1+10^{(\log IC50 - l)\times h}}$$

General Synthetic Experimental

^{1}H NMR spectra were recorded at 300K unless otherwise specified using a Bruker Avance DPX 300, DPX 400 and DPX 500 NMR spectrometer at a frequency of 400.2 and 500.2 MHz respectively. ^{1}H NMR chemical shifts are reported in parts per million (ppm) and are referenced to solvent residual signals: $CDCl_3$ δ 7.26, MeOD δ 3.31, $(CD_3)_2CO$ δ 2.05, DMSO δ 2.50. ^{1}H NMR data is reported as chemical shift (δ_H), relative integral, multiplicity (s = singlet, d = doublet, t = triplet, q = quartet, dd = doublet of doublets, ddd = doublet of doublet of doublets, tt = triplet of triplets, qd = quartet of doublets), coupling constant (*J* Hz) and assignment where possible. Numbering of carbons and protons is shown in Figure S1 (Supplementary Information). Low resolution mass spectra were recorded on a Finnigan LCQ Deca ion trap mass spectrometer (ESI). High resolution mass spectra were recorded on a Bruker 7T Fourier Transform Ion Cyclotron Resonance Mass Spectrometer (FTICR).

Melting points were recorded using a Stanford Research Systems OptiMelt Automated Melting Point System. Infrared (IR) absorption spectra were recorded on a Bruker ALPHA Spectrometer with Attenuated Total Reflection (ATR) capability, using OPUS 6.5 software. Optical rotations were measured using a POLAAR 2001 polarimeter and $[\alpha]_D^{20}$ values are reported in 10^{-1} deg cm^2 g^{-1}.

Preparative reverse phase HPLC was performed using a Waters 600 Multisolvent Delivery System and Waters 500 pump with a Waters 2996 photodiode array detector or Waters 490E programmable wavelength detector operating at 254 and 280 nm. A Waters Sunfire 5 µm, 19 x 150 mm column was used at a flow rate of 7 mL min^{-1}. Preparative HPLC was performed at a flow rate of 7 mL min^{-1}. Compounds were eluted with 0.1% TFA in water (solvent A), and 0.1% TFA in CH_3CN (solvent B) using a linear gradient of 0-100% B over 40 min.

LC-MS was performed on a Shimadzu LC-MS 2020 instrument consisting of a LC-M20A pump and a SPD-20A UV/Vis detector coupled to a Shimadzu 2020 mass spectrometer (ESI) operating in positive mode. Separations were performed on a Waters Sunfire 5 µm, 2.1 x 150 mm column (C18), operating at a flow rate of 0.2 mL min^{-1}. Separations were performed using a mobile phase of 0.1% formic acid in water (Solvent A) and 0.1% formic acid in acetonitrile (Solvent B) and a linear gradient of 0-100% B over 30 min or 0-50% B over 30 min.

Materials

Analytical thin layer chromatography (TLC) was performed on commercially prepared silica plates (Merck Kieselgel 60 0.25 mm F254). Flash column chromatography was performed using 230-400 mesh Kieselgel 60 silica eluting with distilled solvents as described. Ratios of solvents used for TLC and column chromatography are expressed in v/v as specified. Compounds were visualised by UV light at 254 nm or using vanillin or cerium molybdate stain. Commercial materials were used as received unless otherwise noted. DCM and methanol were distilled from calcium hydride, and THF and diethyl ether were distilled over sodium/benzophenone. Anhydrous DMF was purchased from Sigma-Aldrich.

2-(3,4-Dimethoxyphenyl)-6-morpholino-4H-chromen-4-one (8). To a solution of 4,5-dimethoxyanthranilic acid **7** (1.0 g, 5.1 mmol) in methanol (4 mL) was added trimethyl orthoformate (2.20 mL, 20.3 mmol) and ammonium acetate (1.56 g, 20.3 mmol). The reaction was heated at 120 ºC for 3 h. The reaction was allowed to cool to room temperature, water (40 mL) was added and the suspension was stirred for an additional 1 h. The solution was subsequently filtered to afford **8** as a white solid (900 mg, 86%). m.p. 283-284 ºC (decomp.). IR (ATR): ν = 2837, 1645, 1606 cm^{-1}. ^1H NMR (400 MHz, DMSO-d_6): δ 7.96 (1H, s, Ar-H, H-2), 7.43 (1H, s, Ar-H, H-5), 7.08 (1H, s, Ar-H, H-8), 3.90 (3H, s, OCH_3), 3.85 (3H, s, OCH_3). ^{13}C NMR (75 MHz, DMSO-d_6): δ 160.3, 154.4, 148.5, 144.8, 143.8, 115.6, 107.9, 104.9, 55.9, 55.7. LRMS [M+H^+] 207.0. These data are in agreement with those previously reported by VanBrocklin *et al*.[24]

4-Chloro-6,7-dimethoxyquinazoline (9). A mixture of quinazoline **8** (0.44 g, 2.0 mmol) and phosphorus(V) oxychloride (4.4 mL, 43 mmol) was refluxed for 5 h. Solvent was removed *in vacuo* and the residue was dissolved in dichloromethane (200 mL) and washed with saturated aqueous $NaHCO_3$ solution (3 × 50 mL) and brine (50 mL). The organic layer was dried over anhydrous $MgSO_4$ and the solvent was removed *in vacuo* to afford a crude residue that was purified by column chromatography (95:5 v/v CH_2Cl_2: MeOH) to afford **9** as a white solid (310 mg, 70%). m.p. 186-188 ºC. IR (ATR): ν = 1683 cm^{-1}. ^1H NMR (400 MHz, $CDCl_3$): δ 8.87 (1H, s, Ar-H, H-2), 7.39 (1H, s, Ar-H, H-5), 7.33 (1H, s, Ar-H, H-8), 4.07 (6H, s, 2 × OCH_3). ^{13}C NMR (101 MHz, $CDCl_3$): δ 159.1, 156.8, 152.5, 151.5, 149.1, 119.6, 106.9, 102.7, 56.6, 56.4. LRMS [M+H^+] 225.0. These data are in agreement with those previously reported by VanBrocklin *et al*.[23]

General procedure 1: synthesis of aminoquinazoline-based inhibitors 10-12, **22**, **32-42.** To a solution of 4-Chloro-6,7-dimethoxyquinazoline **9** (0.07-1.33 mmol) in isopropanol (11.2-25.7 mL/mmol) was added 1,2-diaminocyclohexane, piperazine hydrochloride hydrate, 1,4-phenylenediamine or the corresponding 4-aminocarboxamides (0.07-5.63 mmol, 1-12 eq.) and the reaction mixture was heated at 120 ºC for 3-5 h. The reaction was subsequently filtered and washed with diethyl ether (2 × 10 mL) to obtain compounds **10-12**, **22-33** which were purified by column chromatography, reverse phase HPLC or used without further purification as specified.

General procedure 2: Synthesis of aminoquinazoline-based inhibitors 14-19. To a stirring solution of amine **10-12** (0.26-0.31 mmol) in DMF (58 mL/mmol) was added benzoic acid, cyclohexanecarboxylic acid or Boc-L-hydroxyproline-OH (1.1 eq.), *N*,*N*-diisopropylethylamine (1-1.6 eq.) and HATU (1.6 eq.). The reaction mixture was allowed to stir at room temperature for 4-20 h at which point it was diluted with ethyl acetate (30 mL), washed with water (4 × 10 mL), brine (10 mL) and dried over anhydrous $MgSO_4$. The solvent was removed *in vacuo* to give a crude residue that was purified by column chromatography or reverse phase HPLC to afford compound **14-19**.

***N*^{1}-(6,7-dimethoxyquinazolin-4-yl)cyclohexane-1,2-diamine (10).** 4-Chloro-6,7-dimethoxyquinazoline **9** (300 mg, 1.33 mmol) was added to a solution of 1,2-diaminocyclohexane (0.65 mL, 5.33 mmol) in isopropanol (15 mL) according to general procedure 1. Following column chromatography (9:1 v/v CH_2Cl_2: MeOH) compound **10** was afforded as a yellow solid (234 mg, 60%). m.p. 123-126 ºC. ^1H NMR (400 MHz, DMSO-d_6): δ 9.37 (1H, d, *J* 8.2 Hz, NH), 8.75 (1H, s, Ar-H, H-2), 8.07 (2H, br. s, NH_2), 7.88 (1H, s, Ar-H, H-8), 7.35 (1H, s, Ar-H, H-5), 4.59-4.54 (1H, m, H-1'), 3.98 (6H, s, OCH_3), 3.40 (1H, t, *J* 11.4 Hz, H-2'), 2.16 (1H, *app.* dd, *J* 13.3, 4.1 Hz, H-3'), 2.01 (1H, *app.* d, *J* 12.8 Hz, H-6'), 1.83-1.79 (2H, m, H-5'), 1.65-1.54 (2H, m, H-3' + H-6'), 1.38-1.32 (2H, m, H-4'). ^{13}C NMR (101 MHz, DMSO-d_6): δ 158.8, 154.3, 153.5, 148.6, 146.3, 109.4, 107.1, 103.9, 57.0, 56.1, 52.9, 52.5, 31.5, 30.3, 24.7, 24.3. LRMS [M+H^+] 303.2. HRMS (ESI) m/z cald for $C_{16}H_{23}N_4O_2$ [M+H^+]: 303.1816, found 303.1817.

6,7-dimethoxy-4-(piperazin-1-yl)quinazoline (11). 4-Chloro-6,7-dimethoxyquinazoline **9** (300 mg, 1.33 mmol) was added to a solution of piperazine hexahydrate (1.03 g, 5.32 mmol) in isopropanol (15 mL) according to general procedure 1 for 3 h. The reaction was subsequently diluted with dichloromethane (100 mL), washed with brine (2 × 40 mL) and dried over anhydrous Na_2SO_4. The solvent was removed *in vacuo* to give a residue that was purified by column chromatography (9:1 v/v CH_2Cl_2: CH_3OH → 4:1 v/v CH_2Cl_2: CH_3OH) to afford compound **11** as a white solid (255 mg, 70%). m.p. 153-154 ºC. IR (ATR): ν = 3235, 2827, 1616 cm^{-1}. ^1H NMR (500 MHz, CD_3OD): δ 8.48 (1H, s, Ar-H, H-2), 7.13 (2H, s, Ar-H, H-5 + H-8), 3.97 (3H, s, OCH_3), 3.95 (3H, s, OCH_3), 3.66 (4H, t, *J* = 5 Hz, H-2'+ H-6'), 3.04 (4H, t, *J* = 5 Hz, H-3' + H-5'). ^{13}C NMR (125 MHz, CD_3OD): δ 163.8, 155.2, 152.0, 148.9, 148.1, 110.9, 105.7, 103.2, 55.2, 55.1, 50.1, 44.9. LRMS [M+H^+] 275.1. HRMS (ESI) m/z cald for $C_{14}H_{19}N_4O_2$ [M+H^+]: 275.1503, found 275.1502.

***N*^{1}-(6,7-dimethoxyquinazolin-4-yl)benzene-1,4-diamine (12).** 4-Chloro-6,7-dimethoxyquinazoline **9** (103 mg, 0.46 mmol) was added to a solution of 1,4-phenylenediamine (609 mg, 5.63 mmol) in isopropanol (7.5 mL) according to general procedure 1 to obtain **12** as a yellow solid (120 mg, 89%). m.p. 137-140 ºC (decomp.). IR (ATR): ν = 3333, 1631 cm^{-1}. ^1H NMR (400 MHz, DMSO-d_6): δ 8.32 (1H, s, Ar-H, H-2), 7.81 (1H, s, Ar-H, H-8), 7.29 (2H, d, *J* 8.8 Hz, Ar-H, H-2' + H-6'), 7.13 (1H, s, Ar-H, H-5), 6.60 (2H, d, *J* 8.8 Hz, Ar-H, H-3' + H-5'), 3.94 (3H, s, OCH_3), 3.93 (3H, s, OCH_3). ^{13}C NMR (75 MHz, DMSO-d_6): δ 157.0, 154.2, 152.2, 148.8, 145.6, 127.4, 124.9, 118.3, 113.7, 108.3, 105.6, 102.4, 56.2, 55.8. LRMS [M+H^+] 297.1. These data are in agreement with those previously reported by Garske *et al*.[25]

***N*-(4-((6,7-dimethoxyquinazolin-4-yl)amino)phenyl)cyclohexane carboxamide (13).** To a mixture of cyclohexane carboxylic acid (29 mg, 0.22 mmol) in DMF (1.6 mL) was added *N*,*N*'-diisopropylcarbodiimide (55 µL, 0.35 mmol) and 4-dimethylaminopyridine (43 mg, 0.35 mmol). The solution was allowed to stir at room temperature for 15 min. Amine **12** (60 mg, 0.20 mmol) was then added to the above reaction mixture which was allowed to stir at room temperature for 20 h. The reaction mixture was diluted with ethyl acetate (50 mL), washed with water (5 × 15 mL), brine (15 mL) and dried over anhydrous $MgSO_4$. The solvent was removed *in vacuo* to give a crude residue that was purified by reverse phase HPLC (0 to 100% MeCN over 40 min) to afford compound **13** as a yellow solid (50 mg, 56%). m.p. 222-225 ºC (decomp.). IR (ATR): ν = 2937, 1676 cm^{-1}. ^1H NMR (400 MHz, DMSO-d_6): δ 10.85 (1H, s, NH), 9.97 (1H, s, NH), 8.76 (1H, s, Ar-H, H-2), 8.05 (1H, s, Ar-H, H-8), 7.72 (2H, d, *J* 8.9 Hz, Ar-H, H-2' + H-6'), 7.56 (2H, d, *J* 8.9 Hz, Ar-H, H-3' + H-5'), 7.28 (1H, s, Ar-H, H-5), 4.00 (3H, s, OCH_3), 3.99 (3H, s, OCH_3), 2.35 (1H, tt, *J* 11.6, 3.5 Hz, H-1"), 1.86-1.73 (4H, m), 1.67 (1H, d, *J* 11.7 Hz), 1.43 (2H, qd, *J* 11.4, 9.9, 2.0 Hz), 1.35-1.17 (3H, m). ^{13}C NMR (101 MHz, DMSO-d_6): δ 174.8 (C=O), 158.6, 158.3, 156.5, 150.5, 149.9, 138.0, 132.2, 125.3, 119.6, 107.7, 103.6, 101.4, 57.0, 56.9, 45.3, 29.6, 25.9, 25.7. LRMS [M+H^+] 407.2. HRMS (ESI) m/z cald for $C_{23}H_{27}N_4O_3$ [M+H^+]: 407.2077, found 407.2078.

(4-(6,7-dimethoxyquinazolin-4-yl)piperazin-1-yl)(phenyl)methanone (14). Amine **11** (71 mg, 0.26 mmol) was reacted with benzoic acid (35 mg, 0.29 mmol) in DMF (15 mL) in the presence of *N*,*N*-diisopropylethylamine (70 µL, 0.26 mmol) and HATU (156 mg, 0.40 mmol) for 4 h according to general procedure 2. Purification by column chromatography (9:1 v/v CH_2Cl_2: CH_3OH) provided compound **14** as a white solid (45 mg, 47%). m.p. 221-223 ºC (decomp.). IR (ATR): ν = 2800, 1641 cm^{-1}. ^1H NMR (400 MHz, DMSO-d_6): δ 8.57 (1H, s, Ar-H, H-2), 7.49-7.44 (4H, m, Ar-H), 7.24 (1H, s, Ar-H, H-8), 7.16 (1H, s, Ar-H, H-5), 3.94 (3H, s, OCH_3), 3.92 (3H, s, OCH_3), 3.75-3.56 (8H, m, 4 × CH_2). ^{13}C NMR (101 MHz, DMSO-d_6): δ 169.9 (C=O), 163.3, 155.0, 152.8, 149.2, 148.9, 136.4, 130.0, 128.9, 127.4, 111.1, 107.9, 104.1, 56.4, 56.3, 49.5 (×2). LRMS [M+H^+] 379.4. HRMS (ESI) m/z cald for $C_{21}H_{23}N_4O_3$ [M+H^+]: 379.1765, found 379.1764.

Cyclohexyl(4-(6,7-dimethoxyquinazolin-4-yl)piperazin-1-yl)methanone (15). Amine **11** (71 mg, 0.26 mmol) was reacted with cyclohexane carboxylic acid (38 mg, 0.29 mmol) in DMF (15 mL) in the presence of *N*,*N*-diisopropylethylamine (70 µL, 0.26 mmol) and HATU (156 mg, 0.40 mmol) for 20 h according to general procedure 2. Purification by reverse phase HPLC (0 to 100% MeCN over 40 min) provided compound **15** as a

white solid (50 mg, 50%). m.p. 165-166 ºC (decomp.). IR (ATR): ν = 2936, 2855, 1792, 1772, 1678 cm^{-1}. ^1H NMR (400 MHz, CD_3OD): δ 8.66 (1H, s, Ar-H, H-2), 7.47 (1H, s, Ar-H, H-8), 7.24 (1H, s, Ar-H, H-5), 4.35 (4H, dt, *J* = 10.4, 5.2 Hz, H-3' + H-5'), 4.08 (3H, s, OCH_3), 4.03 (3H, s, OCH_3), 3.88-3.84 (4H, m, H-2'+ H-6'), 2.72 (1H, ddd, *J* 11.3, 8.1, 3.2 Hz, H-1"), 1.86-1.77 (5H, m), 1.56-1.27 (5H, m). ^1H NMR (100 MHz, CD_3OD): δ 176.1 (C=O), 161.9, 157.3, 149.6, 146.2, 137.4, 106.6, 105.8, 98.8, 55.9, 55.6, 44.0, 40.9, 40.2, 29.0, 25.6, 25.3. LRMS [*M*+H^+] 385.1. HRMS (ESI) m/z cald for $C_{21}H_{29}N_4O_3$ [*M*+H^+]: 385.2234, found 385.2232.

***N*-(2-((6,7-dimethoxyquinazolin-4-yl)amino)cyclohexyl)benzamide (16).** Amine **10** (65 mg, 0.21 mmol) was reacted with benzoic acid (28 mg, 0.23 mmol) in DMF (12 mL) in the presence of *N*,*N*-diisopropylethylamine (58 µL, 0.20 mmol) and HATU (126 mg, 0.32 mmol) for 4 h according to general procedure 2. Purification by column chromatography (95:5 v/v CH_2Cl_2: CH_3OH) provided compound **16** as a pale yellow oil (41 mg, 48%). IR (ATR): ν = 2923, 1707 cm^{-1}. ^1H NMR (400 MHz, DMSO-d_6): δ 8.40 (1H, d, *J* 11.0 Hz, NH), 8.38 (1H, s, Ar-H, H-2), 7.76 (1H, s, NH), 7.59 (2H, dd, *J* 7.3, 1.4 Hz, Ar-H, H-2" + H-6"), 7.48 (1H, s, Ar-H, H-8), 7.45-7.38 (1H, m, Ar-H, H-4"), 7.37-7.28 (2H, m, Ar-H, H-3" + H-5"), 7.01 (1H, s, Ar-H, H-5), 4.30 (1H, *app.* dd, *J* 13.6, 7.9 Hz, H-2'), 4.04 (1H, *app.* dd, *J* 12.1, 9.8 Hz, H-1'), 3.89 (3H, s, OCH_3), 3.87 (3H, s, OCH_3), 2.11 (1H, t, *J* 11.4 Hz), 2.02 (1H, *app.* d, *J* 12.7 Hz), 1.78 (2H, *app.* d, *J* 8.7 Hz, CH_2), 1.70-1.42 (2H, m, CH_2), 1.36 (2H, *app.* t, *J* 10.3 Hz, CH_2). ^{13}C NMR (101 MHz, DMSO-d_6): δ 167.1 (C=O), 158.8, 154.3, 153.6, 148.8, 145.8, 134.9, 131.5, 128.6, 127.4, 108.5, 107.1, 102.4, 56.5, 56.1, 54.8, 54.1, 32.2 (×2), 25.2, 25.1. LRMS [*M*+H^+] 407.2. HRMS (ESI) m/z cald for $C_{23}H_{27}N_4O_3$ [*M*+H^+]: 407.2078, found 407.2076.

***N*-(2-((6,7-dimethoxyquinazolin-4-yl)amino)cyclohexyl)cyclohexane carboxamide (17).** Amine **10** (93 mg, 0.31 mmol) was reacted with cyclohexane carboxylic acid (84 µL, 0.48 mmol) in DMF (18 mL) in the presence of *N*,*N*-diisopropylethylamine (58 µL, 0.20 mmol) and HATU (181 mg, 0.48 mmol) for 24 h according to general procedure 2. Purification by column chromatography (98:2 v/v CH_2Cl_2: CH_3OH → 95:5 v/v CH_2Cl_2: CH_3OH) provided compound **17** as a white solid (40 mg, 31%). m.p. 98-100 ºC (decomp.). IR (ATR): ν = 3266, 2934, 2859, 1675, 1636 cm^{-1}. ^1H NMR (400 MHz, CD_3OD): δ 8.60 (1H, s, Ar-H, H-2), 7.86 (1H, d, *J* 6.0 Hz, NH), 7.67 (1H, s, Ar-H, H-8), 7.12 (1H, s, Ar-H, H-5), 4.43 (1H, dt, *J* 11.6, 4.8 Hz, H-2'), 4.05 (3H, s, OCH_3), 4.02 (3H, s, OCH_3), 4.01-3.93 (1H, m, H-1'), 2.20-2.12 (1H, m, H-3'), 2.02-1.93 (2H, m), 1.92-1.83 (2H, m), 1.70-1.40 (8H, m), 1.33-1.15 (2H, m), 1.11-1.01 (3H, m), 0.95 (1H, *app.* dt, *J* 12.0, 3.6 Hz, H-5'). ^{13}C NMR (101 MHz, CD_3OD): δ 178.0 (C=O), 159.5, 157.2, 151.0, 148.3, 134.3, 106.5, 102.7, 98.8, 57.1, 55.8, 55.8, 51.8, 44.8, 31.3, 30.7, 29.2, 28.9, 25.3, 25.2, 25.1, 24.6, 24.3. LRMS [*M*+H^+] 413.2. HRMS (ESI) m/z cald for $C_{23}H_{33}N_4O_3$ [*M*+H^+]: 413.2547, found 413.2546.

(2*S*,4*R*)-*N*-(4-((6,7-dimethoxyquinazolin-4-yl)amino)phenyl)-4-hydroxypyrrolidine-2-carboxamide (19). Amine **12** (74 mg, 0.26 mmol) was reacted with Boc-L-hydroxyproline (97 mg, 0.29 mmol) in DMF (15 mL) in the presence of *N*,*N*-diisopropylethylamine (70 µL, 0.26 mmol) and HATU (156 mg, 0.40 mmol) for 20 h according to general procedure 2 to obtain Boc-carbamate **18** which was used without further purification. To a solution of Boc-carbamate **18** (52 mg, 0.10 mmol) in THF (3 mL) was added 4 M HCl in dioxane (408 µL). The reaction was stirred at room temperature for 16 h at which point the reaction was quenched with saturated aqueous $NaHCO_3$ (10 mL). The mixture was then extracted into ethyl acetate (3 × 50 mL), washed with water, brine and dried over anhydrous $MgSO_4$. The solvent was removed *in vacuo* to give a crude residue that was purified by reverse phase HPLC (0 to 100% MeCN over 40 min) to afford compound **19** (32 mg, 30%) as a yellow amorphous solid. IR (ATR): ν = 3581, 1739, 1724 cm^{-1}. ^1H NMR (400 MHz, CD_3OD): δ 8.67 (1H, s, Ar-H, H-2), 7.98 (1H, s, Ar-H, H-8), 7.77-7.72 (4H, m, Ar-H, H-2' + H-6' + H-3' + H-5'), 7.25 (1H, s, Ar-H, H-5), 4.74-4.57 (2H, m, H-2" + H-4"), 4.09 (3H, s, OCH_3), 4.08 (3H, s, OCH_3), 3.51 (1H, dd, *J* 12.1, 3.5 Hz, H-5"$_{ax}$), 3.39 (1H, dd, *J* 12.5, 1.8 Hz, H-5"$_{eq}$), 2.61 (1H, dd, *J* 13.6, 7.5 Hz, H-3"$_{eq}$), 2.22 (1H, ddd, *J* 14.0, 10.3, 4.0 Hz, H-3"$_{ax}$). ^{13}C NMR (101 MHz, CD_3OD): δ 166.5 (C=O), 158.5, 157.5, 151.4, 148.3, 136.1, 136.0, 133.3, 124.7, 120.0, 107.5, 102.4, 99.4, 69.9, 59.3, 55.9, 55.8, 53.9, 38.7. LRMS [*M*+H^+] 410.0. HRMS (ESI) m/z cald for $C_{21}H_{24}N_5O_4$ [*M*+H^+]: 410.1820, found 410.1823. $[\alpha]_D^{25}$ = +28º (c = 0.1 in CH_3OH)

(*S*)-*N*-(4-((6,7-dimethoxyquinazolin-4-yl)amino)phenyl)pyrrolidine-2-carboxamide (22). 4-Chloro-6,7-dimethoxyquinazoline **9** (100 mg, 0.44 mmol) was reacted with amine **20** (191 mg, 0.44 mmol) in isopropanol (9.6 mL) according to general procedure 1 to obtain Fmoc-carbamate **21** as a yellow solid which was submitted to the next step without purification. A solution of Fmoc-carbamate **21** was treated with 25% piperidine (5 mL) in a mixture of dichloromethane and methanol (1:1, v/v) for 1 h. The solvent was removed *in vacuo* to afford a crude residue that was purified by column chromatography (95: 4: 1 v/v/v CH_2Cl_2: MeOH: Et_3N → 90: 9: 1 v/v/v CH_2Cl_2 : MeOH : Et_3N) to afford compound **22** as an amorphous solid (59 mg, 34% over 2 steps). IR (ATR): ν = 3066, 2986, 1673, 1639 cm^{-1}. ^1H NMR (400 MHz, DMSO-d_6, 330 K): δ 10.59 (1H, s, NH), 8.67 (1H, s, Ar-H, H-2), 8.01 (1H, s, Ar-H, H-8), 7.74-7.66 (4H, m, Ar-H, H-2' + H-6' + H-3' + H-5'), 7.30 (1H, s, Ar-H, H-5), 4.40 (1H, m, H-2"), 3.99 (6H, s, 2× OCH_3), 3.33 (2H, m, H-5"), 2.43 (1H, m, H-3"$_{eq}$), 2.03 (3H, m, H-3"$_{ax}$ + H-4"). ^{13}C NMR (100 MHz, DMSO-d_6, 330 K): δ 167.2 (C=O), 158.7, 156.3, 150.7, 150.4, 140.0, 135.8, 134.4, 124.9, 120.4, 108.3, 103.7, 103.2, 60.4, 57.1, 56.8, 46.4, 30.0, 24.0. LRMS [*M*+H^+] 394.0. HRMS (ESI) m/z cald for $C_{21}H_{24}N_5O_3$ [*M*+H^+]: 394.1874, found 394.1872. $[\alpha]_D^{25}$ = -26º (c = 0.15 in CH_3OH).

***N*-(4-((6,7-dimethoxyquinazolin-4-yl)amino)phenyl)-3-(4-fluoro-phenyl)-5-methylisoxazole-4-carboxamide (23).** 4-Chloro-6,7-dimethoxyquinazoline **9** (90 mg, 0.39 mmol) was reacted with the corresponding 4-aminocarboxamide (124 mg, 0.39 mmol) in isopropanol (8.8 mL) according to general procedure 1 to obtain compound **23** as an off-white solid (140 mg, 72%). m.p. 253-256 ºC (decomp.). IR (ATR): ν = 1659, 1631 cm^{-1}. ^1H NMR (400 MHz, DMSO-d_6): δ 11.45 (1H, s, NH), 10.64 (1H, s, NH), 8.76 (1H, s, Ar-H, H-2), 8.34 (1H, s, Ar-H, H-8), 7.81-7.72 (4H, m, Ar-H, H-2' + H-6' + H-2" + H-6"), 7.66 (2H, d, *J* 8.5 Hz, Ar-H, H-3' + H-5'), 7.42-7.30 (3H, m, Ar-H, H-5, H-3" + H-5"), 4.02 (3H, s, CH_3), 3.99 (3H, s, OCH_3), 2.62 (3H, s, OCH_3); ^{13}C NMR (100 MHz, DMSO- d_6): δ 170.7, 164.8 (C=O), 161.4 (d, *J* 199 Hz, *ipso*-C), 159.9, 158.5, 156.7, 150.6, 149.1, 137.1, 135.9, 133.2, 130.5 (d, *J* 8.7 Hz, *meta*-C), 125.8, 125.0 (d, *J* 3.1 Hz, *para*-C), 120.4, 116.4 (d, *J* 21.8 Hz, *ortho*-C), 113.6, 107.7, 104.5, 100.3, 57.4, 56.9, 12.5. LRMS [*M*+H^+] 500.3. HRMS (ESI) m/z cald for $C_{27}H_{23}FN_5O_4$ [*M*+H^+]: 500.1729, found 500.1728.

***N*-(4-((6,7-dimethoxyquinazolin-4-yl)amino)phenyl)pyrazine-2-carboxamide (24).** 4-Chloro-6,7-dimethoxyquinazoline **9** (50 mg, 0.22 mmol) was reacted with the corresponding 4-aminocarboxamide (109 mg, 0.22 mmol) in isopropanol (3.1 mL) according to general procedure 1 to obtain a crude solid that was purified by reverse-phase HPLC (gradient: 0-100% MeCN over 40 min) to afford compound **24** (TFA salt) as a yellow solid (80 mg, 90%). m.p. 220-224 ºC (decomp.). IR (ATR): ν = 3340, 1686 cm^{-1}. ^1H NMR (500 MHz, DMSO-d_6): δ 10.89 (1H, s, NH), 10.86 (1H, s, NH), 9.30 (1H. d, *J* 1.5 Hz, Ar-H, H-3"), 8.94 (1H, d, *J* 2.5 Hz, Ar-H, H-5"), 8.89-8.82 (1H, m, Ar-H, H-6"), 8.77 (1H, s, Ar-H, H-2), 8.04 (1H, s, Ar-H, H-8), 8.00 (2H, d, *J* 8.9 Hz, Ar-H, H-2' + H-6'), 7.65 (2H, d, *J* 8.9 Hz, Ar-H, H-3' + H-5'), 7.27 (1H, s, Ar-H, H-5), 3.99 (6H, s, 2 × OCH_3); ^{13}C NMR (100 MHz, DMSO-d_6): δ 162.3 (C=O), 158.5, 156.7, 150.7, 150.0, 148.4, 145.6, 144.7, 143.9, 137.4, 136.8, 133.6, 125.5, 121.4, 107.9, 103.8, 101.4, 57.2, 57.1. LRMS [*M*+H^+] 403.3. HRMS (ESI) m/z cald for $C_{21}H_{19}N_6O_3$ [*M*+H^+]: 403.1513, found 403.1514.

***N*-(4-((6,7-dimethoxyquinazolin-4-yl)amino)phenyl)-2-hydroxy benzamide (25).** 4-Chloro-6,7-dimethoxyquinazoline **9** (16 mg, 0.072 mmol) was reacted with the corresponding 4-aminocarboxamide (16 mg, 0.072 mmol) in isopropanol (1.6 mL) according to general procedure 1 to obtain a crude solid that was purified by reverse-phase HPLC (gradient: 0-100% MeCN over 40 min) to afford compound **25** as a yellow solid (9 mg, 30%). m.p. = 213-214 ºC. IR (ATR): ν = 3385, 1703 cm^{-1}. ^1H NMR (400 MHz, Acetone-d_6): δ 9.94 (1H, s, NH), 8.71 (1H, s, Ar-H, H-2),

8.04 (1H, dd, *J* = 8.0, 1.6 Hz, Ar-H, H-6"), 7.96 (1H, s, Ar-H, H-8), 7.87-7.75 (4H, m, Ar-H, H-2' + H-3' + H-5'+ H-6'), 7.68 (1H, s, Ar-H, H-5), 7.47 (1H, ddd, *J* = 8.6, 7.1, 1.6 Hz, Ar-H, H-4"), 7.00 (1H, *app*. d, *J* 8.6 Hz, Ar-H, H-3"), 6.93 (1H, dd, *J* 7.6, 7.1 Hz, Ar-H, H-5"), 4.01 (3H, s, OCH_3), 3.96 (3H, s, OCH_3). ^{13}C NMR (100 MHz, DMSO): δ 166.9 (C=O), 158.8, 158.5, 158.1, 156.4, 150.4, 150.3, 136.3, 134.1, 133.7, 129.5, 125.1, 121.6, 119.5, 118.1, 117.7, 107.9, 103.6, 102.0, 57.0, 56.8. LRMS [*M*+H$^+$] 417.3. HRMS (ESI) m/z cald for $C_{23}H_{21}N_4O_4$ [*M*+H$^+$]: 417.1557, found 417.1560.

***N*-(4-((6,7-dimethoxyquinazolin-4-yl)amino)phenyl)-2-nitro-benzamide (26).** 4-Chloro-6,7-dimethoxyquinazoline **9** (200 mg, 0.86 mmol) was reacted with the corresponding 4-aminocarboxamide (221 mg, 0.86 mmol) in isopropanol (20 mL) according to general procedure 1 to obtain compound **26** as a yellow solid (200 mg, 52%) after filtration and washing with diethyl ether (2 × 10 mL). m.p. 263-265 ºC (decomp.). IR (ATR): ν = 2756, 1679, 1530 cm^{-1}. ^1H NMR (500 MHz, DMSO-d_6): δ 11.37 (1H, s, NH), 10.85 (1H, s, NH), 8.80 (1H, s, Ar-H, H-2), 8.30 (1H, s, Ar-H, H-8), 8.17 (1H, *app*. d, *J* 8.0 Hz, Ar-H, H-3"), 7.90 (1H, dd, *J* 8.0, 7.5 Hz, Ar-H, H-5"), 7.82-7.77 (4H, m, Ar-H, H-2' + H-6' + H-3' + H-5'), 7.68 (2H, m, Ar-H, H-4" + H-6"), 7.36 (1H, s, Ar-H, H-5), 4.02 (3H, s, OCH_3), 3.99 (3H, s, OCH_3). ^{13}C NMR (125 MHz, DMSO-d_6): δ 164.6 (C=O), 158.6, 156.7, 150.6, 149.2, 146.9, 137.4, 136.0, 134.6, 133.0 (×2), 131.5, 129.8, 125.8, 124.8, 120.2, 107.7, 104.3, 100.4, 57.4, 56.9. LRMS [*M*+H$^+$] 446.2. HRMS (ESI) m/z cald for $C_{23}H_{20}N_5O_5$ [*M*+H$^+$]: 446.1459, found 446.1459.

2-amino-*N*-(4-((6,7-dimethoxyquinazolin-4-yl)amino)phenyl) benzamide (27). Compound **26** (45 mg, 0.10 mmol) in ethyl acetate (1.5 mL) was hydrogenated (1 atm) over 10% Pd/C (15 mg) for 16 h. The reaction mixture was subsequently filtered over Celite® and the filtrate concentrated *in vacuo.* Purification by reverse phase HPLC (gradient: 0-100% MeCN over 40 min) provided compound **27** as a yellow solid (12 mg, 29%). m.p. 127-128 ºC (decomp.). IR (ATR): ν = 3452, 1677, 1639 cm^{-1}. ^1H NMR (400 MHz, CD_3OD): δ 8.67 (1H, s, Ar-H, H-2), 7.99 (1H, s, Ar-H, H-8), 7.88-7.77 (2H, m, Ar-H, H-2' + H-6'), 7.71 (2H, d, *J* 8.9 Hz, Ar-H, H-3' + H-5'), 7.67 (1H, dd, *J* = 7.9, 1.5 Hz, Ar-H, H-6"), 7.30 (1H, ddd, *J* 8.5, 7.5, 1.5 Hz, Ar-H, H-4"), 7.22 (1H, s, Ar-H, H-5), 6.93-6.84 (1H, m, Ar-H, H-3"), 6.80 (1H, *app*. t, *J* = 7.5 Hz, Ar-H, H-5"), 4.08 (6H, s, 2 × OCH_3). ^{13}C NMR (101 MHz, CD_3OD): δ 168.7 (C=O), 158.5, 157.6, 151.4, 148.0, 147.8, 137.4, 135.3, 132.5, 132.2, 128.0, 124.5, 121.0, 117.5, 117.2, 117.0, 107.3, 102.5, 99.0, 55.9, 55.8. LRMS [*M*+H$^+$] 416.0. HRMS (ESI) m/z cald for $C_{23}H_{22}N_5O_3$ [*M*+H$^+$]: 416.1717, found 416.1714.

***N*-(4-((6,7-dimethoxyquinazolin-4-yl)amino)phenyl)-4-hydroxy benzamide (28).** 4-Chloro-6,7-dimethoxyquinazoline **9** (21 mg, 0.09 mmol) was reacted with the corresponding 4-aminocarboxamide (32 mg, 0.094 mmol) in isopropanol (2.0 mL) according to general procedure 1 to obtain TBS-protected intermediate as a yellow solid which was used in the next step without purification (50 mg, quant.). To a solution of the TBS-protected intermediate (50 mg, 0.094 mmol) in anhydrous tetrahydrofuran (1 mL) was added tetrabutylammonium fluoride (1 M solution in THF, 0.11 mL, 0.11 mmol) and the reaction was allowed to stir at room temperature for 1 h. The reaction mixture was then diluted with ethyl acetate (60 mL) and washed with saturated aqueous NH_4Cl solution (2 × 30 mL) and brine (30 mL). The organic layer was then dried over anhydrous $MgSO_4$. The solvent was removed *in vacuo* to give a crude residue that purified by reverse-phase HPLC (gradient: 0-100% MeCN over 40 min) to afford compound **28** (TFA salt) as a yellow solid (20 mg, 51% over 2 steps). m.p. 164-165 ºC. IR (ATR): ν = 3009, 1709 cm^{-1}; 1H NMR (400 MHz, DMSO-d_6): δ 10.91 (1H, s, NH), 10.13 (1H, s, NH), 8.77 (1H, s, Ar-H, H-2), 8.08 (1H, s, Ar-H, H-8), 7.93-7.83 (4H, m, Ar-H), 7.62 (2H, d, *J* 8.5 Hz, Ar-H, H-3' + H-5'), 7.30 (1H, s, Ar-H, H-5), 6.88 (2H, d, *J* 8.2 Hz, Ar-H, H-4" + H-5"), 3.99 (6H, s, 2 × OCH_3). ^{13}C NMR (100 MHz, DMSO-d_6): δ 165.6 (C=O), 161.1, 158.3, 156.5, 150.5, 149.9, 138.0, 137.3, 132.6, 130.2, 125.7, 125.2, 120.8, 115.4, 107.7, 103.7, 101.3, 57.1, 56.9. LRMS [*M*+H$^+$] 417.1. HRMS (ESI) m/z cald for $C_{23}H_{21}N_4O_4$ [*M*+H$^+$]: 417.1557, found 417.1557.

***N*-(4-((6,7-dimethoxyquinazolin-4-yl)amino)phenyl)-4-fluoro-benzamide (29).** 4-Chloro-6,7-dimethoxyquinazoline **9** (100 mg, 0.44 mmol) was reacted with the corresponding 4-aminocarboxamide (102 mg, 0.44 mmol) in isopropanol (9.6 mL) according to general procedure 1. Purification by reverse phase HPLC (gradient: 0-100% MeCN over 40 min) provided compound **29** as a yellow solid (12 mg, 29%). m.p. 257-260 ºC (decomp.). IR (ATR): ν = 1636 cm^{-1}. 1H NMR (400 MHz, DMSO-d_6): δ 10.89 (1H, s, NH), 10.41 (1H, s, NH), 8.77 (1H, s, Ar-H, H-2), 8.09-8.03 (3H, m, Ar-H, H-8, H-2" + H-6"), 7.87 (2H, d, *J* 8.6 Hz, Ar-H, H-2' + H-6'), 7.65 (2H, d, *J* 8.6 Hz, Ar-H, H-3' + H-5'), 7.39 (2H, *app*. t, *J* 8.6 Hz, Ar-H, H-3" + H-5"), 7.27 (1H, s, Ar-H, H-2), 3.99 (6H, s, 2× OCH_3). ^{13}C NMR (100 MHz, DMSO-d_6): δ 165.8 (C=O), 165.0 (d, *J* 161 Hz, *ipso*-C), 158.7, 158.3, 156.5, 150.5, 149.9, 137.5, 133.0, 131.7 (d, *J* 3.4 Hz, *para*-C), 130.8 (d, *J* 9.2 Hz, *meta*-C), 125.3, 121.1, 115.8 (d, *J* 22 Hz, *ortho*-C), 107.7, 103.6, 101.3, 57.0, 56.9. LRMS [*M*+H$^+$] 419.4. HRMS (ESI) m/z cald for $C_{23}H_{20}FN_4O_3$ [*M*+H$^+$]: 419.1514, found 419.1513.

***N*-(4-((6,7-dimethoxyquinazolin-4-yl)amino)phenyl)-3-hydroxy benzamide (30).** 4-Chloro-6,7-dimethoxyquinazoline **9** (54 mg, 0.24 mmol) was reacted with the corresponding 4-aminocarboxamide (54 mg, 0.24 mmol) in isopropanol (5.6 mL) according to general procedure 1. Purification by reverse phase HPLC (gradient: 0-100% MeCN over 40 min) provided compound **30** as a yellow solid (39 mg, 39%). m.p. 181-182 ºC (decomp.). IR (ATR): ν = 3474, 1675 cm^{-1}. ^1H NMR (500 MHz, DMSO-d_6): δ 10.71 (1H, br. s), 10.28 (1H, s, NH), 9.78 (1H, br. s), 8.74 (1H, s, Ar-H, H-2), 8.04 (1H, s, Ar-H, H-8), 7.87 (2H, d, *J* 8.7 Hz, Ar-H, H-2' + H-6'), 7.64 (2H, d, *J* 8.7 Hz, Ar-H, H-3' + H-5'), 7.40 (1H, d, *J* 7.7 Hz, Ar-H, H-6"), 7.35-7.33 (2H, m, Ar-H, H-2" + H-5"), 7.26 (1H, s, Ar-H, H-5), 6.99 (1H, dd, *J* = 8.0, 2.5 Hz, Ar-H, H-4"), 3.99 (6H, s, 2 × OCH_3). ^{13}C NMR (125 MHz, DMSO-d_6): δ 166.0 (C=O), 158.5, 158.2, 157.8, 156.3, 150.4, 150.3, 137.4, 136.8, 133.2, 129.9, 125.0, 120.9, 119.0, 118.6, 115.0, 107.9, 103.5, 102.1, 57.0, 56.8. LRMS [*M*+H$^+$] 417.3. HRMS (ESI) m/z cald for $C_{23}H_{21}N_4O_4$ [*M*+H$^+$]: 417.1557, found 417.1558.

***N*-(4-((6,7-dimethoxyquinazolin-4-yl)amino)phenyl)-3-methoxy benzamide (31).** 4-Chloro-6,7-dimethoxyquinazoline **9** (72 mg, 0.32 mmol) was reacted with the corresponding 4-aminocarboxamide (78 mg, 0.32 mmol) in isopropanol (7.4 mL) according to general procedure 1 to obtain compound **31** (90 mg, 65%) as a yellow solid after filtration and washing with diethyl ether (2 × 10 mL). m.p. 187-190 ºC (decomp.). IR (ATR): ν = 2952, 1674 cm^{-1}. ^1H NMR (400 MHz, DMSO-d_6): δ 11.11 (1H, s, NH), 10.36 (1H, s, NH), 8.78 (1H, s, Ar-H, H-2), 8.24 (1H, s, Ar-H, H-8), 7.89 (2H, d, *J* = 8.4 Hz, Ar-H, H-2' + H-6'), 7.67 (2H, d, *J* 8.4 Hz, Ar-H, H-3' + H-5'), 7.57 (1H, *app*. d, *J* 7.7 Hz, 1H, Ar-H, H-6"), 7.52 (1H, s, Ar-H, H-2"), 7.46 (1H, *app*. t, *J* 7.9 Hz, Ar-H, H-5"), 7.32 (1H, s, Ar-H, H-5), 7.17 (1H, dd, *J* = 8.0, 2.5 Hz, Ar-H, H-4"), 4.01 (3H, s, OCH_3), 3.99 (3H, s, OCH_3), 3.85 (3H, s, OCH_3). ^{13}C NMR (101 MHz, DMSO-d_6): δ 165.7 (C=O), 159.7, 158.4 (×2), 156.6, 150.6, 149.5, 137.6, 136.7, 133.0, 130.1, 125.4, 121.0, 120.4, 117.8, 113.5, 107.8, 104.2, 100.9, 57.3, 56.9, 55.9. LRMS [*M*+H$^+$] 417.3. HRMS (ESI) m/z cald for $C_{23}H_{21}N_4O_4$ [*M*+H$^+$]: 417.1557, found 417.1560.

***N*-(4-((6,7-dimethoxyquinazolin-4-yl)amino)phenyl)-3-nitro-benzamide (32).** 4-Chloro-6,7-dimethoxyquinazoline **9** (160 mg, 0.69 mmol) was reacted with the corresponding 4-aminocarboxamide (177 mg, 0.69 mmol) in isopropanol (16 mL) according to general procedure 1 to obtain compound **32** (TFA salt) as a yellow solid (300 mg, 98%) after filtration and washing with diethyl ether (2 × 10 mL). m.p. 140-144 ºC (decomp.). IR (ATR): ν =1673, 1640 cm^{-1}. ^1H NMR (500 MHz, DMSO-d_6): δ 10.69 (1H, s, NH), 8.79 (1H, t, *J* 2.0 Hz, Ar-H, H-2"), 8.71 (1H, s, Ar-H, H-2), 8.44 (1H, dd, *J* 8.2, 2.0 Hz, Ar-H, H-4"), 8.43 (1H, dd, *J* 8.0, 1.5 Hz, Ar-H, H-6"), 8.04 (1H, s, Ar-H, H-8), 7.88-7.84 (3H, m, Ar-H, H-2' + H-6' + H-5"), 7.68 (2H, d, *J* 9.0 Hz, Ar-H, H-3' + H-5'), 7.25 (1H, s, Ar-H, H-5), 3.98 (3H, s, OCH_3), 3.97 (3H, s, OCH_3). ^{13}C NMR (126 MHz, DMSO-d_6): δ 164.1 (C=O), 158.4, 156.6, 150.6, 150.3, 148.4, 138.0, 136.9, 136.7, 134.7, 133.8, 130.9, 126.9, 125.3, 122.9, 121.5, 108.0, 103.6, 101.9, 57.1, 57.0. LRMS [*M*+H$^+$] 446.2. HRMS (ESI) m/z cald for $C_{23}H_{20}N_5O_5$ [*M*+H$^+$]: 446.1459, found 446.1459.

3-amino-*N*-(4-((6,7-dimethoxyquinazolin-4-yl)amino)phenyl) benzamide (33). Compound **32** (61 mg, 0.13 mmol) in methanol (10 mL) was hydrogenated (1 atm) over 10% Pd/C (13 mg) for 24 h. The reaction mixture was subsequently filtered over Celite® and the filtrate concentrated *in vacuo* to afford a crude solid that was purified by reverse phase HPLC (gradient: 0-100% MeCN over 40 min) to afford compound **33** as a yellow solid (16 mg, 30%). m.p. 121-123 ºC (decomp.). IR (ATR): ν = 1735, 1697 cm^{-1}. ^{1}H NMR (400 MHz, DMSO-d_6): δ 11.06 (1H, s, NH), 10.24 (1H, s, NH), 8.80 (1H, s, Ar-H, H-2), 8.08 (1H, s, Ar-H, H-8), 7.87 (2H, d, *J* 8.5 Hz, Ar-H, H-2' + H-6'), 7.61 (2H, d, *J* 8.5 Hz, Ar-H, H-3' + H-5'), 7.28 (1H, s, Ar-H, H-5), 7.20-7.15 (3H, m, Ar-H), 6.81 (1H, *app.* d, *J* 8.0 Hz, Ar-H, H-4"), 4.00 (6H, s, 2 × OCH_3). ^{13}C NMR (101 MHz, DMSO-d_6): δ 166.8 (C=O), 158.5, 156.7, 150.6, 149.6, 148.3, 138.1, 136.3, 132.5, 129.3, 125.5, 120.8, 118.0, 116.0, 115.7, 114.0, 107.6, 103.8, 100.8, 57.1, 57.0. LRMS [*M*+H^+] 416.3. HRMS (ESI) m/z cald for $C_{23}H_{22}N_5O_3$ [*M*+H^+]: 416.1717, found 416.1717.

3-(cyanomethoxy)-*N*-(4-((6,7-dimethoxyquinazolin-4-yl)amino) phenyl)benzamide (34). Compound **30** (20 mg, 0.048 mmol), bromoacetonitrile (3.7 µL, 0.053 mmol) and cesium carbonate (39 mg, 0.12 mmol) in anhydrous acetonitrile (1 mL) was heated at 80 ºC for 1 h. The reaction was subsequently filtered and the solvent was removed *in vacuo* to afford a crude residue that was purified by reverse phase HPLC (0 to 100% MeCN over 40 min) to afford compound **34** (TFA salt) as a yellow solid (12 mg, 55%). m.p. 141-144 ºC. IR (ATR): ν = 2954, 2365, 1672 cm^{-1}. ^{1}H NMR (500 MHz, DMSO-d_6): δ 10.39 (1H, s, NH), 8.76 (1H, s, Ar-H, H-2), 8.04 (1H, s, Ar-H, H-8), 7.89-7.87 (2H, m, Ar-H, H-2' + H-6'), 7.71-7.63 (4H, m, Ar-H, H-3' + H-5', H-2" + H-6"), 7.56 (1H, t, *J* = 8.0 Hz, Ar-H, H-5"), 7.33 (1H, dd, *J* = 8.2, 2.7 Hz, Ar-H, H-4"), 7.27 (1H, s, Ar-H, H-5), 5.28 (2H, s, CH_2), 3.99 (6H, 2 × OCH_3). ^{13}C NMR (126 MHz, DMSO-d_6): δ 165.2 (C=O), 158.5, 158.2, 156.8, 156.4, 150.4, 150.2, 137.3, 137.0, 133.3, 130.4, 125.1, 122.2, 121.0, 118.45, 116.9, 114.7, 107.9, 103.6, 101.8, 57.0, 56.8, 54.2. LRMS [*M*+H^+] 456.3. HRMS (ESI) m/z cald for $C_{25}H_{22}N_5O_4$ [*M*+H^+]: 456.1666, found 456.1666.

2-(3-((4-((6,7-dimethoxyquinazolin-4-yl)amino)phenyl) carbamoyl)phenoxy)acetic acid (35). Compound **30** (60 mg, 0.14 mmol), *tert*-butyl bromoacetate (28 µL, 0.19 mmol) and cesium carbonate (118 mg, 0.36 mmol) in anhydrous acetonitrile (3 mL) was heated at 50 ºC for 3 h. The reaction was subsequently filtered and the solvent was removed *in vacuo* to afford a crude residue that was dissolved in a mixture of trifluoroacetic acid in dichloromethane (300 µL, 1:1 v/v). The reaction was stirred at room temperature for 16 h. The solvent was removed *in vacuo* to give a crude residue that was purified by reverse phase HPLC (0 to 100% MeCN over 40 min) to afford compound **35** as a yellow solid (10 mg, 14% over 2 steps). m.p. 236-239 ºC (decomp.). IR (ATR): ν = 3365, 1679, 1631 cm^{-1}. ^{1}H NMR (500 MHz, DMSO-d_6): δ 10.32 (1H, s, NH), 8.61 (1H, s, Ar-H, H-2), 7.98 (1H, s, Ar-H, H-8). 7.83 (1H, d, *J* 8.5 Hz, Ar-H, H-3' + H-5'), 7.70 (2H, d, *J* 8.5 Hz, H-2' + H-6'), 7.59 (1H, *app.* d, *J* 8.0 Hz, Ar-H, H-6"), 7.51-7.50 (1H, m, Ar-H, H-2"), 7.46-7.43 (1H, m, Ar-H, H-5"), 7.27 (1H, s, Ar-H, H-5), 7.14 (1H, dd, *J* 8.5, 2.5 Hz, Ar-H, H-4"), 4.78 (2H, s, CH_2), 3.97 (3H, s, OCH_3), 3.95 (3H, s, OCH_3). ^{13}C NMR (126 MHz, DMSO-d_6): δ 170.5 (C=O), 165.4 (C=O), 158.8, 158.2, 157.7, 155.6, 151.4, 149.9, 136.6, 136.4, 134.3, 130.0, 124.3, 121.1, 120.8, 118.2, 114.1, 108.5, 104.2, 103.1, 65.1, 56.8, 56.6. LRMS [*M*+Na^+] 496.9. HRMS (ESI) m/z cald for $C_{25}H_{23}N_4O_6$ [*M*+H^+]: 475.1612, found 475.1612.

Acknowledgements

We would like to thank the Australian National Health and Medical Research Council (NHMRC project grant 1011266) and the John A. Lamberton Research Scholarship and Australian Postgraduate Award for PhD funding (ATT). Finally, we would also like to thank Dr. Alexandra Manos-Turvey for providing the mycobacterial cell wall diagram (PhD thesis, The University of Sydney, 2012) used in Figure 1.

Notes and References:

1. A. Koul, E. Arnoult, N. Lounis, J. Guillemont and K. Andries, *Nature*, 2011, **469**, 483.
2. World Health Organization, Global Tuberculosis control: W.H.O. report 2012.
3. A. M. Ginsberg and M. Spigelman, *Nat. Med*., 2007, **13**, 290.
4. A. Zumla, P. Nahid and S. Cole, *Nat. Rev. Drug Disc*., 2013, **12**, 388.
5. L. G. Dover and G. D. Coxon, *J. Med. Chem*., 2011, **54**, 6157.
6. R. Gupta, M. Lavollay, J.-L. Mainardi, M. Arthur, W. Bishai and G. Lamichhane, *Nat. Med*., 2010, **16**, 466.
7. C. Walsh, *Nat. Rev. Microbiol*., 2003, **1**, 65.
8. L. Tremblay, F. Fan and J. Blanchard, *Biochemistry*, 2010, **49**, 3766.
9. J.-E. Hugonnet, L. Tremblay, H. Boshoff, C. Barry and J. Blanchard, *Science*, 2009, **323**, 1215.
10. S. T. Cole, R. Brosch, J. Parkhill, T. Garnier, C. Churcher, D. Harris, S. V. Gordon, K. Eiglmeier, S. Gas, C. E. Barry, F. Tekaia, K. Badcock, D. Basham, D. Brown, T. Chillingworth, R. Connor, R. Davies, K. Devlin, T. Feltwell, S. Gentles, N. Hamlin, S. Holroyd, T. Hornsby, K. Jagels, A. Krogh, J. McLean, S. Moule, L. Murphy, K. Oliver, J. Osborne, M. A. Quail, M. A. Rajandream, J. Rogers, S. Rutter, K. Seeger, J. Skelton, R. Squares, S. Squares, J. E. Sulston, K. Taylor, S. Whitehead and B. G. Barrell, *Nature*, 1998, **393**, 537.
11. Z. Zhang, E. M. M. Bulloch, R. D. Bunker, E. N. Baker and C. J. Squire, *Acta Crystallogr. D*, 2009, **65**, 275.
12. S. Verma, M. Jaiswal, N. Kumar, A. Parikh, V. Nandicoori and B. Prakash, *Acta Crystallogr. F*, 2009, **65**, 435.
13. I. Mochalkin, S. Lightle, Y. Zhu, J. F. Ohren, C. Spessard, N. Y. Chirgadze, C. Banotai, M. Melnick and L. McDowell, *Protein Sci*., 2007, **16**, 2657.
14. N. A. Larsen, T. J. Nash, M. Morningstar, A. B. Shapiro, C. Joubran, C. J. Blackett, A. D. Patten, P. A. Boriack-Sjodin and P. Doig, *Biochem. J*., 2012, **446**, 405.
15. M. Urbaniak, I. Collie, W. Fang, T. Aristotelous, S. Eskilsson, O. Raimi, J. Harrison, I. Navratilova, J. Frearson, D. van Aalten and M. Ferguson, *ACS Chem. Biol.*, 2013, **DOI:** 10.1021/cb400411x.
16. I. Mochalkin, S. Lightle, L. Narasimhan, D. Bornemeier, M. Melnick, S. VanderRoest and L. McDowell, *Protein Sci*., 2008, **17**, 577.
17. V. Singh, K. Das and K. Seshadri, *PloS One*, 2012, **7**, e43969.
18. M. Webb, *Proc. Natl. Acad. Sci. U.S.A.,* 1992, **89**, 4884.
19. A. Gehring, W. Lees, D. Mindiola, C. Walsh and E. Brown, *Biochemistry*, 1996, **35**, 579.
20. S. E. Thomas, S. Aine, Y. Yulin and J. C. Stuart, *Med. Chem. Commun*., 2012, **3**, 735.
21. E. C. Dykhuizen, J. F. May, A. Tongpenyai and L. L. Kiessling, *J. Am. Chem. Soc.*, 2008, **130,** 6706.
22. S. G. Franzblau, R. S. Witzig, J. C. McLaughlin, P. Torres, G. Madico, A. Hernandez, M. T. Degnan, M. B. Cook, V. K. Quenzer, R. M. Ferguson, R. H. Gilman, *J. Clin. Microbiol.* 1998, **36**, 362.
23. F. W. Studier, *Protein Expres. Purif.,* 2005, **41**, 207.
24. H. VanBrocklin, J. Lim, S. Coffing, D. Hom, K. Negash, M. Ono, J. Gilmore, I. Bryant and D. Riese, *J. Med. Chem.*, 2005, **48**, 7445.
25. A. Garske, U. Peters, A. Cortesi, J. Perez and K. Shokat, *Proc. Natl. Acad. Sci. U.S.A.,* 2011, **108**, 15046.